High spectral purity laser system for the AURIGA detector optical readout

Livia Conti

Dipartimento di Fisica, Università di Padova, and INFN, Sezione di Padova

Via Marzolo 8, I-35131 Padova, Italy

Maurizio De Rosa and Francesco Marin

Dipartimento di Fisica, Università di Firenze, INFN, Sezione di Firenze, and LENS

Via Sansone 1, I-50019 Sesto Fiorentino (FI), Italy

conti@lnl.infn.it, derosa@lens.unifi.it, marin@fi.infn.it

We describe a low frequency noise laser system conceived for the readout of small mechanical vibrations. The system consists of a Nd:YAG source stabilized to a high Finesse Fabry-Perot cavity and achieves the best performance in the range 1–10 kHz, with a minimum residual noise of 4×10^{-3} Hz/$\sqrt{\text{Hz}}$. We perform an extended characterization of the frequency stability by means of an independent optical cavity and we also measure the residual fluctuations after transmission through an optical fiber. Our apparatus is optimized for the use in an optical readout for the gravitational wave detector AURIGA, where a laser system with the characteristics here reported will allow an improvement of one order of magnitude in the detector sensibility.

OCIS codes: 120.3940, 120.2230, 000.2780.

1. Introduction

An important task for precision metrology is monitoring extremely small vibrations. The recent and still increasing progresses in opto-electronics, in particular concerning laser stabilization and high quality optical components, have boosted the possibility of using such techniques for measuring displacements. The most demanding applications concern the detection of gravitational waves (GW),[1] which is one of the most challenging tasks in nowadays Physics. The application of opto-mechanical transducers to resonant bar detectors of GW was theoretically studied by Kulagin *et al.* .[2] J.-P. Richard and coworkers investigated in details such systems,[3,4] performed preliminary works on suitable Fabry–Perot cavities and also tested an opto-mechanical transducer at room temperature.[5] The basic idea is to compare the vibration of an optical cavity sensitive to the bar motion to that of a stable reference cavity, by means of resonant laser radiation. Together with resonant bar detectors, the present ground-based GW detection strategy implies the use of large interferometers.[6] Even in this case, several accelerometers and displacement detectors are included in the experimental apparatus and the use of electro-optical techniques for small vibration transducers can be of great interest.[7] Such equipments require a frequency-stabilized laser whose radiation must be delivered to the measurement position.

In this work we present a laser system expressly conceived for an opto-mechanical transducer to be installed in the AURIGA ultra-cryogenic GW bar detector.[8] The proposed apparatus is described in Ref. 9. A complete optical readout has been recently experimented on a room temperature bar identical to the one of the ultra-cryogenic detector.[10] The required sensitivity to be competitive with the present status of AURIGA is at least 10^{-18} m/$\sqrt{\text{Hz}}$ in a small bandwidth (about 100 Hz) around the bar fundamental resonance of about 1 kHz, where the bar detector has its peak sensitivity. This requirement implies the use of a laser system with very low frequency noise in the acoustic region, around the detection frequency.

The studies on laser frequency stabilization reported in the literature usually concentrate on the long term stability, measured in the time domain. Very interesting results have been obtained for laser systems stabilized on cryogenic reference cavities,[11] above all for integration times between 1 s and 100 s, thanks to the negligible drift of the sapphire spacers at low temperature. On shorter time-scale, i.e., between 0.01 s and 1 s, the best stability is reported, at our knowledge, by Young *et al.*[12] who also obtain a linewidth below

1 Hz.

In our case, it is more significant to evaluate the system characteristics from the laser frequency noise spectrum rather than from a time resolved analysis. From this point of view, good results have already been obtained with a dye laser by Dirscherl *et al.*,[13] mainly in the range 1-10 kHz. More recently, Musha *et al.*[14] have reported on the dual-locking of a laser source to an optical cavity and a molecular absorption, in order to provide both short- and long-term stabilization. A lower frequency noise in the acoustic region has been achieved with a Nd:YAG laser by a group working for the GW interferometric detector VIRGO.[15] Their results benefit from a very particular and specific experimental equipment: the whole experiment is placed inside a vacuum tank and suspended from a double pendulum VIRGO seismic filter; moreover, the Fabry-Perot cavities have a particular 'truncated football shape' geometry. Even lower residual frequency fluctuations are reported in Ref. 16. The authors use a 10 m long Fabry–Perot interferometer whose 2.8 kg mirrors are suspended as double pendulums to further reduce the frequency noise of a pre-stabilized Nd:YAG laser down to 2×10^{-5} Hz/$\sqrt{\text{Hz}}$ around 1 kHz. The system presented here, while maintaining valuable characteristics concerning the frequency noise in the acoustic range, is a table-top apparatus implemented with standard equipments and can be easily reproduced for a general use in optical vibration detectors.

A critical test we have made concerns the coupling and transmission of the laser radiation through an optical fiber. This is necessary for the implementation of the AURIGA opto-mechanical readout, since the laser radiation must be delivered to the cryogenic bar. Moreover, it is very useful for any handy vibration transducer and, in general, when low-noise radiation must be conveyed to some part of the experimental apparatus. The effect of the transmission through fibers has been considered by some authors,[17] but we could not find in the literature any systematic study of the frequency noise spectrum in these conditions. Even if we are mainly interested in the frequency noise spectral density around 1 kHz, we complete here the characterization of the system with an analysis on a broader spectral region and also estimate its time stability.

2. Description of the system

The system is composed of a phase-modulated laser source and two equal Fabry-Perot cavities: one for the laser stabilization and the other for monitoring the residual frequency fluctuations. An optical fiber can be

inserted in the optical path towards one cavity. All the components are placed on the same table and the two cavities have their optical axes laying on the horizontal plane and one orthogonal to the other.

The scheme of the experimental setup is shown in Fig. 1. The light source is a commercial cw 100 mW Nd:YAG laser based on a non-planar ring geometry (Lightwave mod. 126-1064-100). Tunability is provided in two ways by the laser control box: a *slow* voltage input acts on the laser temperature with a gain of about 5 GHz/V and a time constant of a few seconds; a *fast* voltage input acts on the crystal by means of a piezoelectric actuator with a tuning coefficient of about 3.5 MHz/V and a bandwidth of about 30 kHz.

After a 40 dB optic isolator, two electro-optic modulators (EOM) are contained in a temperature stabilized aluminum box. EOM1 is used with a polarizer in an amplitude stabilization loop. EOM2 is a resonant modulator working at 13.3 MHz which applies a phase modulation with a depth of about 1 rad when driven by a radio frequency (RF) power of 21 dBm.

A first 50% beamsplitter selects part of the radiation which is used for the amplitude stabilization, whose detailed description is reported in Ref. 18. The detected signal, after appropriate electronics, is sent to EOM1 which works as amplitude modulator. In this way, the amplitude noise around 1 kHz is reduced from 23 dB above shot-noise level down to 5 dB. The purpose of the amplitude stabilization is to reduce the effect of radiation pressure and photo-thermal fluctuations in the sensing Fabry-Perot, but it is can be disregarded in the present work.

The laser beam is divided by a second 50% beamsplitter whose two outputs are directed towards different cavities. The optical paths include mode-matching lenses and the power impinging on each cavity is about 10 mW. For part of the measurements, the beam going to the first cavity (C1) is coupled to a single-mode, polarization maintaining optical fiber. This fiber is composed of two 1-meter long patchcords with pigtailed collimators for input and output, and an intermediate 10-meter long fiber, connected by means of standard FC/PC components.

The coupling efficiency of the incoming radiation to the cavity TEM_{00} mode is typically 85-90%. The alignment is very stable and it only needs slight adjustments roughly once a week. After the passage through the optical fiber, the laser beam has a better spatial quality and the coupling to the TEM_{00} mode is $\sim$95%. The Fabry-Perot cavities are made by a 10 cm diameter, 20 cm long Zerodur spacer with optically contacted,

fused silica mirrors. The input mirrors have higher transmission (100 ppm nominal), since the under-coupled cavity provides a better signal for the FM-sidebands technique. The actual mirror quality is limited by contamination during operation and it is different for the two cavities. The characteristics of mirrors and cavities are reported in Table 1, as deduced from the reflection and transmission signals.

Each cavity is set on a double-stage cantilever mechanical suspension machined from a single piece of Al2024. The vertical mechanical isolation is greater than 80 dB at 1 kHz. Cavity and basement are contained in a thermally stabilized, 40 cm diameter vacuum chamber composed of a 11 cm high aluminum base, an aluminum tube with optical windows, and a 4 cm thick aluminum cap with electric and vacuum feedthroughs. Separated vacuum systems, equipped with ion pumps, are used for the two cavities. The vacuum chamber, resting on nylon legs, is enclosed on a cubic, 60 cm side, thermally insulating box made with Plexiglas and lined with 3 cm thick rock wool. The temperature is measured by thermistors on the vacuum chamber and on the Zerodur cylinder. Nine cartridge heaters, with a maximum heating capacity of 540 W, are inserted in the chamber base and cap. The temperature of each cavity can be varied from room temperature up to about 100°C, allowing a coarse tuning of the Fabry-Perot resonance frequency by exploiting the thermal expansion of the spacer. It is then stabilized through a proportional-integral-derivative (PID) control system driven by a PC and a multifunction digital board. The proportional gain is 14000 W/°C, with PID time constants of 1200 s and 2400 s. Fig. 2 shows the monitoring of the cavity temperature for several days of operation. The temperature stability (one standard deviation) is about 10^{-4} °C, measured on the cavity both with the in-loop thermistor and with an independent probe.

C1 can be finely tuned by a system of piezoelectric actuators (PZT) and Invar rods, shown in Fig. 3, which compresses the Zerodur spacer. The effect of the PZT thickness variations is shared between the Invar rods and the Zerodur spacer, proportionally to the inverse of the section area and of the Young modulus. This mechanism allows to reduce the influence of the PZT fluctuations on the cavity length by a factor of 100 and thus minimizes the effect of the PZT thermal and electronic noise. At the same time, the Fabry–Perot resonance can be adjusted within a range of few tens of kHz by driving the PZT with low voltage electronics. A double stage, low-pass filter, with a cutoff frequency of 3 Hz, is set before the PZT to further reduce the electronic noise.

Before each cavity we have placed an optical circulator, formed by a polarizing beam splitter and a quarter-wave plate, which allows to collect the laser beam reflected by the cavity and detect it with a photodiode. A complete characterization of the photo-detection and of the laser noise is reported in Ref. 18. The RF signal from the photodetectors, around 13.3 MHz, is demodulated in a mixer, according to the FM sidebands technique,[19] and low-pass filtered. The local oscillators are provided by commercial signal generators phase-locked to the main oscillators. We obtain a Pound–Drever signal with a slope at resonance of about 10^{-3} V/Hz. The signal from C1 is simply amplified and low-pass filtered. Additional filters are used for the analysis, as specified in the following section.

The Pound–Drever signal from the second cavity (C2) is used as error signal in a feedback loop for locking the laser. A cross-over splits the low- and high-frequency parts of the error signal. The former signal (below 0.1 Hz) is integrated and fed to the *slow* input of the laser control box. The fast signal servo loop electronics consists of a first, pre-locking block with lower gain and wider bandwidth, and a second block composed of three low-pass stages which provides the maximum gain below $\sim$1 kHz. The sum of the two blocks acts on the laser through the *fast* input of the control box. The asymptotic Bode diagram of the loop electronics is shown in Fig. 4 and more details can be found in Ref. 20. The overall servo loop has a 0 dB frequency of 30 kHz and a gain of 120 dB at 1 kHz.

The main interest of this work is focused on the frequency noise spectrum around 1 kHz. For such measurements, we use an anti-aliasing band-pass filter between 500 Hz and 5 kHz. The signal (i.e., the demodulated RF signal either from C1 or C2) is then acquired by a digital scope, with a sampling rate of 500 MS/s. Built-in data analysis procedures of the scope give the power spectrum of the signal and allow averaging on several acquisitions in order to improve the precision of the measurements. The calibration of the vertical scale, from voltage to frequency, is performed using the measured slope of the FM sidebands signal. We have checked this calibration up to 5 kHz by imposing a known, small sinusoidal modulation to the laser frequency and measuring the effect on the Pound-Drever signal. The accuracy of the calibration is about 20%.

For investigating the long-term stability we have acquired the signal by means of a 12 bit analog-to-digital converter (ADC) on a PC board, with a sampling rate of 10 kS/s and a dynamic range of $\pm$10 V,

with an input gain variable from 1 to 100. In this case, an anti-aliasing, low-pass filter of 4th order at 2.3 kHz has been used before the ADC input.

3. Results and discussion

In Fig. 5 we report the frequency noise spectra of the free-running laser (a) and of the laser locked to C2 (b).[21] Both spectra are referred to the same cavity C2 that is used for stabilizing the laser. We also report in the figure the noise spectrum measured after the mixer with the laser far from resonance (trace c). This is given by the sum of electronic noise and laser amplitude noise and it represents a lower limit for the residual frequency noise of the laser when locked to the cavity. The signal in trace (c), around 1 kHz, is just $\sim$ 3 dB above the laser shot noise, that gives the lower limit attainable in classical experiments. The in-loop signal (b) is below trace (c) in the range 100 Hz–1 kHz, demonstrating that the feedback loop provides the necessary gain in the frequency region of interest.

Some narrow peaks are present at multiple frequencies of 50 Hz below 1 kHz, due to the power line. The detectors and the following electronics are powered by batteries, except for the RF oscillator, and most of the peaks observed in the signal are due to the scope itself. The few other narrow spikes are beat notes between the phase-locked oscillators, as we have verified by mixing just the signals from the different generators.

In order to obtain a reliable estimation of the residual laser frequency fluctuations, we use the signal from C1 as discriminator. The laser light, frequency locked to C2, and C1 are brought into resonance by tuning the temperature of the cavities and the PZT of C1. The laser can be maintained locked to C2 and resonant with C1 for long periods (several hours) by applying a slow correction to the PZT voltage, using the Pound–Drever signal from C1 as error signal. In this way, we obtain a noise spectrum which is reported in Fig. 6 (trace a). If we assume that the fluctuations in the length of the two cavities are not correlated, the signal in trace (a) represents an upper limit to the laser frequency noise. The frequency fluctuations of the locked laser with respect to the second cavity are originated, at least, by the sum of three independent contributions corresponding to the two far-from-resonance signals (for the two cavities) and to the in-loop signal (trace (c) in Fig. 6). The measured laser frequency noise is about 9 dB higher than this limit around 1 kHz, due to excess $\sim 1/f$ noise whose origin is presently under investigation. The minimum spectral density is about 4×10^{-3} Hz/$\sqrt{\text{Hz}}$, measured around 4 kHz. Above this frequency the spectrum increases again, due

to the low servo-loop gain.

An important task for this work is to verify whether the passage through the single-mode fiber deteriorates the spectral purity of the locked laser. The noise spectrum for this configuration is reported in Fig. 7, together with the expected noise calculated from the far-from-resonance and in-loop spectra. If we consider the 20% accuracy in the spectra calibration, we cannot appreciate any difference in the frequency noise spectrum between the in-fiber and the in-air propagation, except for a different distribution of some narrow peaks which are due to acoustic disturbances. A detailed view of the spectrum at lower frequencies is shown in Fig. 8, for the two experimental configurations corresponding to in-fiber and in-air propagation. These spectra have been obtained by performing a Fast Fourier Transform algorithm on the data acquired for the long-term analysis. The two spectra are very similar and no extra-noise is added by the fiber. The most relevant structure in the noise spectrum is a strong peak at 57 Hz. This peak is due to a mechanical resonance of the optical table, as we have verified with the help of accelerometers. No attempt has been made to establish more precisely why this resonance influences the measured laser frequency noise, however Doppler and Sagnac effects are obvious candidates for the transfer of mechanical noise to the laser frequency.

Even if it is not relevant to the purposes of the AURIGA opto-mechanical transducer, we have completed the system characterization with a wide-band analysis. Above 4 kHz, the laser frequency noise is determined by the limited loop gain. More interesting is the long-term stability, measured by means of the PC board. For the following measurements we have applied no feedback to the PZT and the data acquisition took place just while the laser was resonant with C1 thanks to the cavities passive stability. A time-series $x(t)$ of the relative frequency is acquired and the data analysis in this case includes the evaluation of the low-frequency noise spectrum and of the Allan variance,[22] defined as

$$\sigma_A^2(\tau) = \frac{1}{N-1} \sum_{k=1}^{N-1} \frac{(\bar{x}_{k+1} - \bar{x}_k)^2}{2} ,$$

where the time-series $x(t)$ is divided into N countiguous intervals of duration τ, and

$$\bar{x}_k(\tau) = \frac{1}{\tau} \int_{(k-1)\tau}^{k\tau} x(t)\, dt$$

is the average of x in the k-th interval.

The data reported in Fig. 9 correspond to two different experimental situations, namely with (open

circles) and without (closed circles) an offset voltage applied to the PZT. The 57 Hz peak, and a few others at lower frequency, determine the Allan deviation $\sigma_A(\tau)$ below 10 s. A completely flat noise level of 10^{-2} Hz/$\sqrt{\text{Hz}}$ would yield a very low Allan deviation of $7 \times 10^{-3}\ \tau^{1/2}$ Hz (where τ is given in seconds), while our minimum measured deviation is about 50 Hz around 10^{-1} s and 10^{-3} s. Above 0.1 s, when a voltage is applied to the PZT, the frequency stability is deteriorated by fluctuations in the applied voltage, in spite of the mechanical reduction system described above. No such effect is observable in the noise spectra: the excess fluctuations are limited to the long term range. We have also completely removed the PZT and the mechanical reduction system, without observing any further decrease of the frequency fluctuations. The operation without PZT implies very long waiting times to force the cavities into resonance acting only on the temperature. The resonance condition is then maintained for a few tens of minutes since the temperature control is not fast enough to compensate the frequency fluctuations. On the contrary, the PZT allows a less accurate temperature adjustment (by more then one order of magnitude) and the resonance condition can be kept indefinitely.

Above 100 s, the Allan deviation increases as $\sigma_A(\tau) = 3\,\tau$. This trend is due to a drift which affects the length of the cavities, corresponding to about 3 Hz/s in the difference between the resonance frequencies, observed over a period of several weeks. During these measurements the cavities are kept at 40°C and 23°C respectively and the corresponding measured thermal expansion coefficients are 2×10^{-8}°C^{-1} and 4×10^{-8}°C^{-1}. The temperature stability of 10^{-4}°C should guarantee frequency fluctuations below 2 kHz, i.e., in a period of one week we should not observe drifts larger than 4×10^{-3} Hz/s. The observed drift is well above this limit and is probably due to long-term relaxations of the Zerodur.[23]

4. Conclusions

We have presented a frequency stabilized laser system to be used in high sensitivity interferometers. Our system represents a trade-off between high performances and ease of implementation. Indeed, it does not involve cryogenic cavities, nor huge and sophisticated mechanical isolation systems and it is probably the most stable laser source obtained in a table-top experiment. As a further, important feature the laser is coupled to a single-mode optical fiber, which is a fundamental characteristics for most applications. In our knowledge, this is the first characterization of the frequency noise characteristics of a fiber-coupled laser

system.

Our system is particularly conceived for the optical readout to be used in the AURIGA ultra-cryogenic GW detector. For this reason, it is focused on the frequency stability around 1 kHz. In particular, the stabilized laser exhibits a frequency noise below 10^{-2} Hz/$\sqrt{\text{Hz}}$ between 1 kHz and 10 kHz. A broader range characterization shows a noise spectral density still below 10^{-1} Hz/$\sqrt{\text{Hz}}$ for frequencies above 100 Hz, except for some narrow resonances, and a best relative Allan deviation of 2×10^{-13} around 10^{-1} s and 10^{-3} s.

A standard implementation of this laser system in a sensitive displacement measurement or in an accelerometer implies the use of a sensing Fabry–Perot cavity. This cavity should be designed without any tuning option, in order to limit the noise, and its Free-Spectral-Range is thus limited by the tuning range of the laser. For a Nd:YAG source, the typical tuning range is about 30 GHz and the sensing cavity cannot be shorter than 5 mm. Our laser system thus allows a sensitivity of about 10^{-19} m/$\sqrt{\text{Hz}}$ between 1 kHz and 10 kHz. In particular, if we consider the opto-mechanical transducer described in Refs. 9, 10 and the parameters of the AURIGA cryogenic detector, the frequency noise of 6×10^{-3} Hz/$\sqrt{\text{Hz}}$ around 1 kHz allows a minimum detectable GW pulse of $h_{\min} = 4 \times 10^{-20}$ with a useful -6 dB bandwidth of about 50 Hz. These figures represent a significant improvement with respect to the present status,[24] characterized by a sensitivity $h_{\min} = 4 \times 10^{-19}$ and a bandwidth of about 2 Hz. The results here reported are particularly important since AURIGA already reached the best sensitivity among the operating GW detectors and optical readout systems can be very useful for advanced GW massive detectors.

Acknowledgements

The work is partially funded by MURST (research program *Transducer systems for cryogenic resonant detectors of gravitational waves*).

References

1. For a comprehensive review of the most recent results of GW research see the special issue of Class. Quant. Grav. **19**, 1227–2049 (2002).

2. V.V. Kulagin, A.G. Polnarev, and V.N. Rudenko, "A combined optical-acoustical gravitational antenna," Sov. Phys. JEPT **64**, 915–921 (1986).

3. J.-P. Richard, "Laser instrumentation for one-phonon sensitivity and wide bandwidth with multimode gravitational radiation detectors," J. Appl. Phys. **64**, 2202–2205 (1988).

4. J.-P. Richard, "Approaching the quantum limit with optically instrumented multimode gravitational-wave bar detectors," Phys. Rev. D **46**, 2309–2317 (1992).

5. Y. Pang and J.-P. Richard, "Room-temperature tests of an optical transducer for resonant gravitational wave detectors," Appl. Opt. **34**, 4982–4988 (1995).

6. A. Giazotto, "Interferometric detection of gravitational waves," Phys. Rep. **182**, 365–424 (1989).

7. N. Mio and K. Tsubono, "Vibration trasducer using an ultrashort Fabry–Perot cavity," Appl. Opt. **34**, 186–189 (1995).

8. G.A. Prodi, L. Conti, R. Mezzena, S. Vitale, L. Taffarello, J.-P. Zendri, L. Baggio, M. Cerdonio, A. Colombo, V. Crivelli-Visconti, R. Macchietto, P. Falferi, M. Bonaldi, A. Ortolan, G. Vedovato, E. Cavallini, and P. Fortini, "Initial operation of the gravitational wave detector AURIGA," in Gravitational Waves, edited by E. Coccia *et al.*, Proceedings of the second Edoardo Amaldi Conference. World Scientific 1998, pp. 148-158. For more information, see also http://www.auriga.lnl.infn.it.

9. L. Conti, M. Cerdonio, L. Taffarello, J. P. Zendri, A. Ortolan, C. Rizzo, G. Ruoso, G. A. Prodi, S. Vitale, G. Cantatore, and E. Zavattini, "Optical transduction chain for gravitational wave bar detectors," Rev. Sci.

Instrum. **69**, 554–558 (1998).

10. M. De Rosa, L. Baggio, M. Cerdonio, L. Conti, G. Galet, F. Marin, A. Ortolan, G. A. Prodi, L. Taffarello, G. Vedovato, S. Vitale, and J. P. Zendri, "First room temperature operation of the AURIGA optical readout," Class. Quant. Grav. **19**, 1919–1924 (2002).

11. S. Seel, R. Storz, G. Ruoso, J. Mlynek, and S. Schiller, "Cryogenic optical resonator: a new tool for laser frequency stabilisation at the 1 Hz level," Phys. Rev. Lett. **78**, 4741–4744 (1997).

12. B. C. Young, F. C. Cruz, W. M. Itano, and J. C. Bergquist, "Visible laser with subhertz linewidths", Phys. Rev. Lett. **82**, 3799–3802. (1999).

13. J. Dirscherl, B. Neizert, T. Wegener and H. Walther, "Visible lasers with subhertz linewidths," Opt. Commun. **91**, 131–139 (1992).

14. M. Musha, T. Kanaya, K. Nakagawa, K. Ueda, " The short- and long-term frequency stabilization of an injection-locked Nd:YAG laser in reference to a Fabry–Perot cavity and an iodine saturated absorption line," Opt. Commun. **183**, 165–173 (2000).

15. F. Bondu, P. Fritschel, C. N. Man, and A. Brillet, "Ultrahigh-spectral-purity laser for the VIRGO experiment," Opt. Lett. **21**, 582–584 (1996).

16. D. A. Clubley, K. D. Skeldon, B. W. Barr, G. P. Newton, K. A. Strain, J. Hough, "Ultrahigh level of frequency stabilisation of an injection locked Nd:YAG laser with relevance to gravitational wave detection," Opt. Commun. **186**, 177–184 (2000).

17. L.-S. Ma, P. Jungner, J. Ye, and J. Hall, "Delivering the same optical frequency at two places: accurate cancellation of phase noise introduced by optical fiber or other time-varying path," Opt. Lett. **19**, 1777–1779 (1994).

18. L. Conti, M. De Rosa and F. Marin, "Low-amplitude-noise laser for AURIGA detector optical readout," Appl. Opt. **39**, 5732–5738 (2000).

19. R. W. P. Drever, J. L. Hall, F. Kowalski, J. Hough, G. M. Ford, A. J. Mulney, and H. Ward, "Laser phase frequency stabilization using an optical resonator," Appl. Phys. B **31**, 97–105 (1983).

20. L. Conti, "An optical readout for the AURIGA resonant gravitational wave detector," PhD Thesis, University of Trento, (1999), http://www.auriga.lnl.infn.it/publications/publications.html.

21. All the spectra reported in this work are one-sided, i.e., reported to positive frequencies.

22. D. W. Allan, "Statistics of atomic frequency standards," Proceedings of the IEEE, **54**, 221–230 (1966).

23. J. Hall, "Frequency stabilized lasers – a driving force for new spectroscopies". In Frontiers in Laser Spectroscopy, Proceedings of the International School of Physics "Enrico Fermi": Course 120, edited by T.W. Hansch and M. Inguscio. North-Holland, Amsterdam, 1994.

24. J.-P. Zendri, L. Baggio, M. Bignotto, M. Bonaldi, M. Cerdonio, L. Conti, M. De Rosa, P. Falferi, P. L. Fortini, M. Inguscio, A. Marin, F. Marin, R. Mezzena, A. Ortolan, G. A. Prodi, E. Rocco, F. Salemi, G. Soranzo, L. Taffarello, G. Vedovato, A. Vinante, and S. Vitale, "Status report and near future prospects for the gravitational wave detector AURIGA," Class. Quant. Grav. **19**, 1925–1933 (2002).

List of Figures

1 Experimental setup. OI: optical isolator; HW: half-wave plate; QW: quarter-wave plate; EOM#: electro-optic modulator; P: polarizer; BS: beam-splitter; PD: photodiode; C#: Fabry–Perot cavity; PBS: polarizing beam-splitter; L: lens; OF: optical fiber, which can be inserted in the path to C1. Dashed lines mark out active thermal stabilization. 16

2 Residual temperature fluctuations of a stabilized Zerodur cavity. Upper curve: from the probe used in the servo-loop. Lower curve: from an independent probe. The difference in the average values is within the calibration accuracy. 17

3 Sketch of the piezoelectric actuators and mechanical de-multiplier used to finely tune the cavity C1. 18

4 Asymptotic Bode diagrams of the frequency loop electronics for the first pre-locking block (dashed line) and for the second locking block (solid line). 19

5 (a) Frequency noise spectral density of the free-running laser. (b) Noise spectrum of the in-loop signal for the laser locked to C2. (c) Noise measured with the laser far from resonance. Frequency resolution: 2 Hz. 20

6 (a) Residual frequency noise of the laser when locked to C2, measured with respect to C1. (b) Noise spectrum measured on the C1 detector when the laser is far from resonance. (c) In-loop spectrum. Frequency resolution: 2 Hz. The dashed line shows the trend of a $1/f$ power noise. 21

7 (a) Frequency noise of the laser after the passage through the single-mode optical fiber. (b) Lower limit to the frequency fluctuations (see text). Frequency resolution: 2 Hz. 22

8 Laser frequency noise: (a) in-air propagation; (b) in-fiber propagation. Frequency resolution: 0.6 Hz. 23

9 Allan deviation of the stabilized laser. Closed circles: with no voltage applied to the PZT. Open circles: with offset voltage applied. The scale on the right gives the relative Allan deviation: σ_A/ν_L, where $\nu_L = 2.82 \times 10^{14}$ Hz is the laser frequency. 24

Table 1. Parameters of the two cavities.

Cavity	C1		C2	
Length (m)	0.2		0.2	
FSR (MHz)	750		750	
Finesse	17000		36000	
Input power (mW)	10		7	
Mirror	in	out	in	out
Radius of curvature (m)	1	1	∞	1

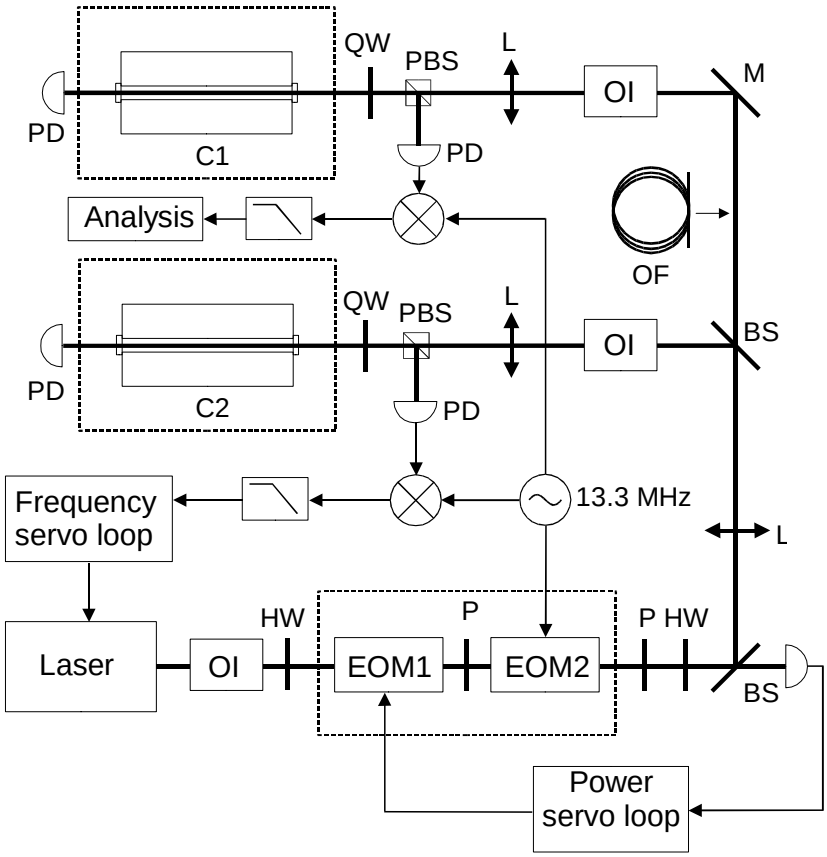

Fig. 1. Experimental setup. OI: optical isolator; HW: half-wave plate; QW: quarter-wave plate; EOM#: electro-optic modulator; P: polarizer; BS: beam-splitter; PD: photodiode; C#: Fabry–Perot cavity; PBS: polarizing beam-splitter; L: lens; OF: optical fiber, which can be inserted in the path to C1. Dashed lines mark out active thermal stabilization.

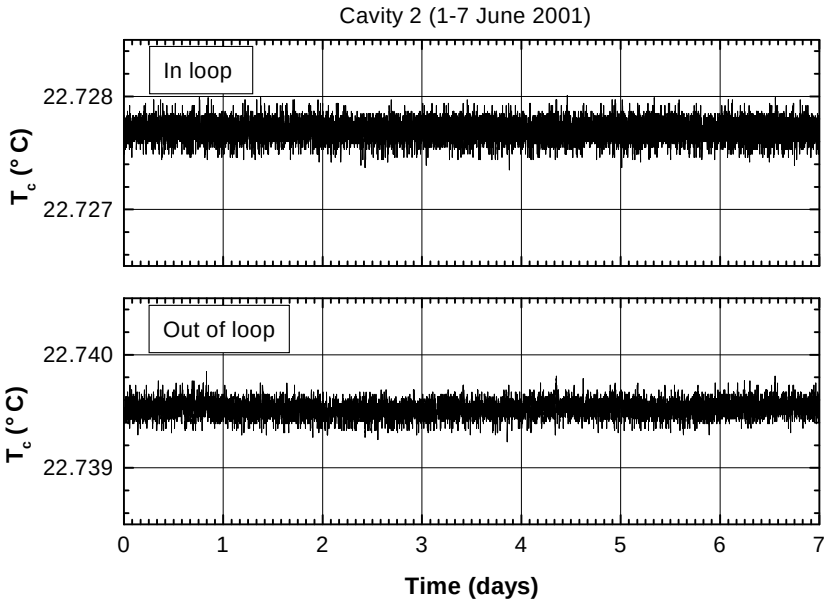

Fig. 2. Residual temperature fluctuations of a stabilized Zerodur cavity. Upper curve: from the probe used in the servo-loop. Lower curve: from an independent probe. The difference in the average values is within the calibration accuracy.

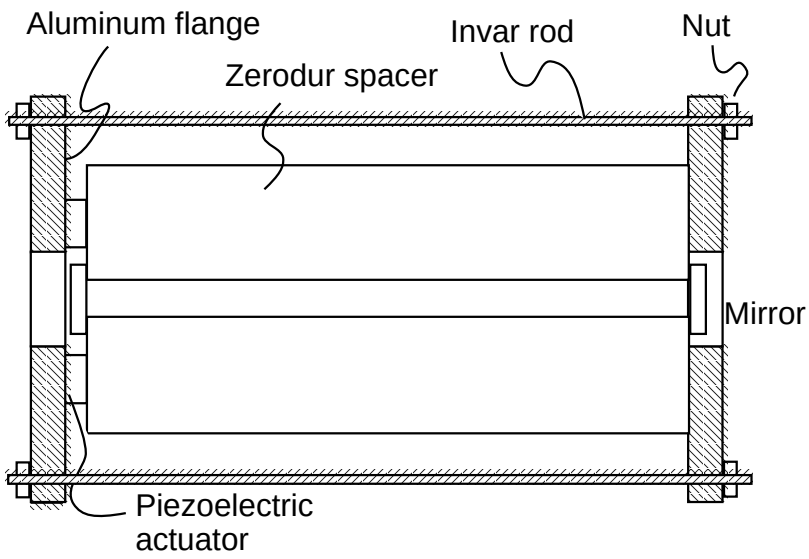

Fig. 3. Sketch of the piezoelectric actuators and mechanical de-multiplier used to finely tune the cavity C1.

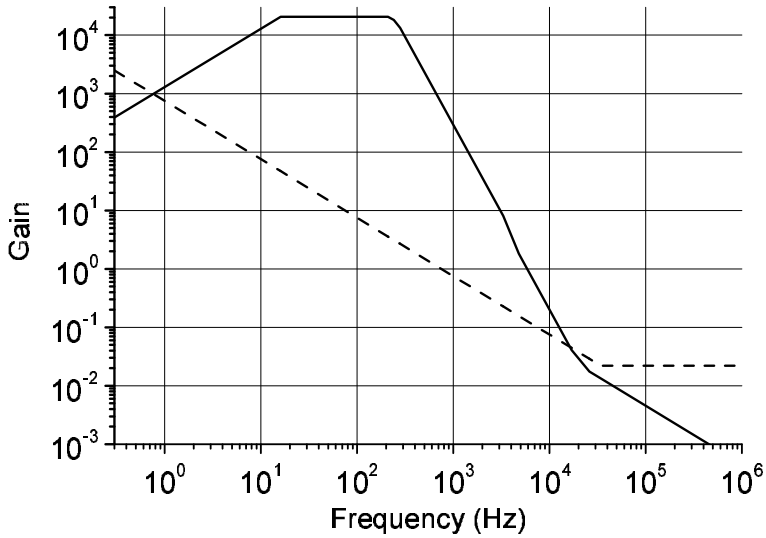

Fig. 4. Asymptotic Bode diagrams of the frequency loop electronics for the first pre-locking block (dashed line) and for the second locking block (solid line).

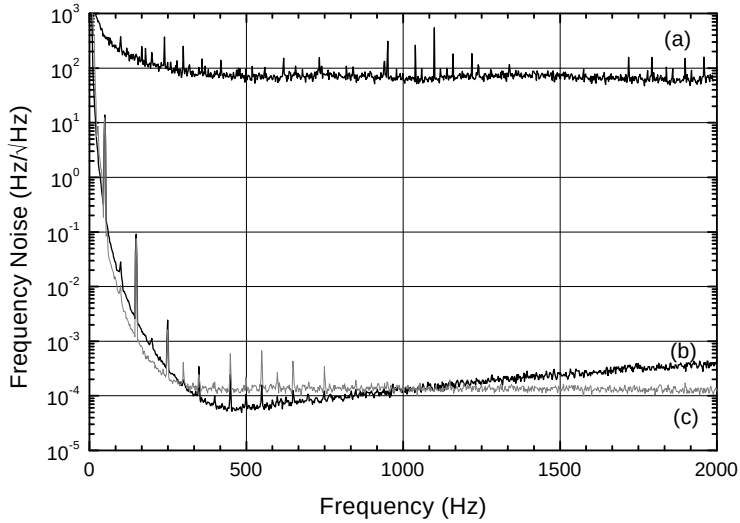

Fig. 5. (a) Frequency noise spectral density of the free-running laser. (b) Noise spectrum of the in-loop signal for the laser locked to C2. (c) Noise measured with the laser far from resonance. Frequency resolution: 2 Hz.

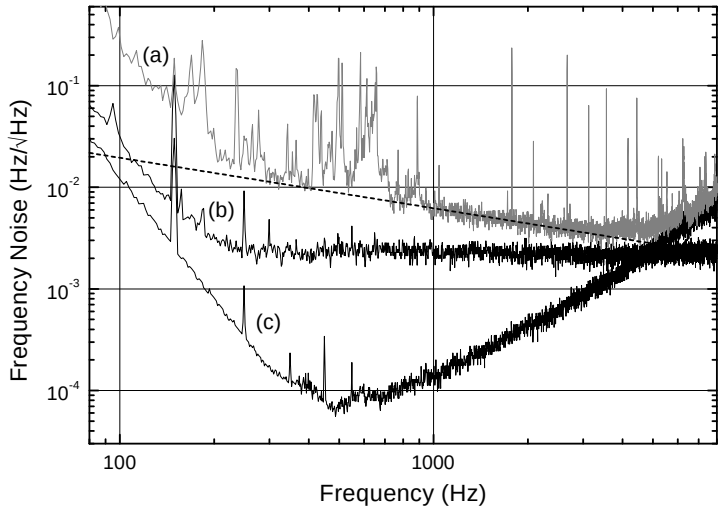

Fig. 6. (a) Residual frequency noise of the laser when locked to C2, measured with respect to C1. (b) Noise spectrum measured on the C1 detector when the laser is far from resonance. (c) In-loop spectrum. Frequency resolution: 2 Hz. The dashed line shows the trend of a $1/f$ power noise.

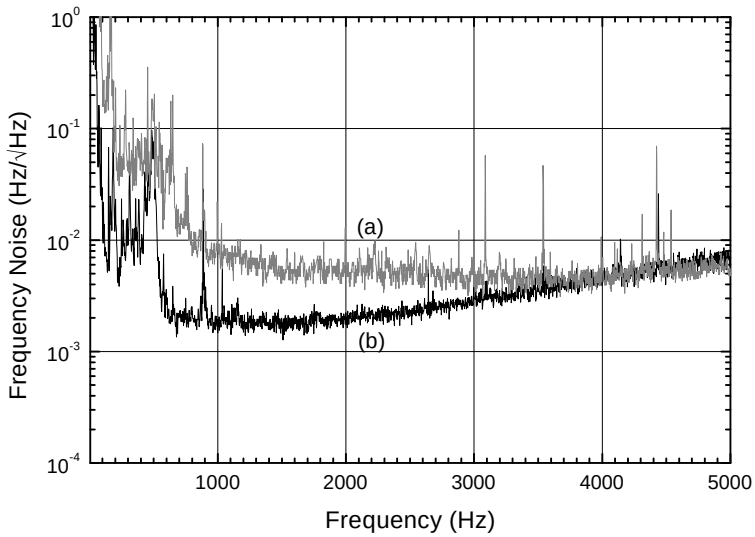

Fig. 7. (a) Frequency noise of the laser after the passage through the single-mode optical fiber. (b) Lower limit to the frequency fluctuations (see text). Frequency resolution: 2 Hz.

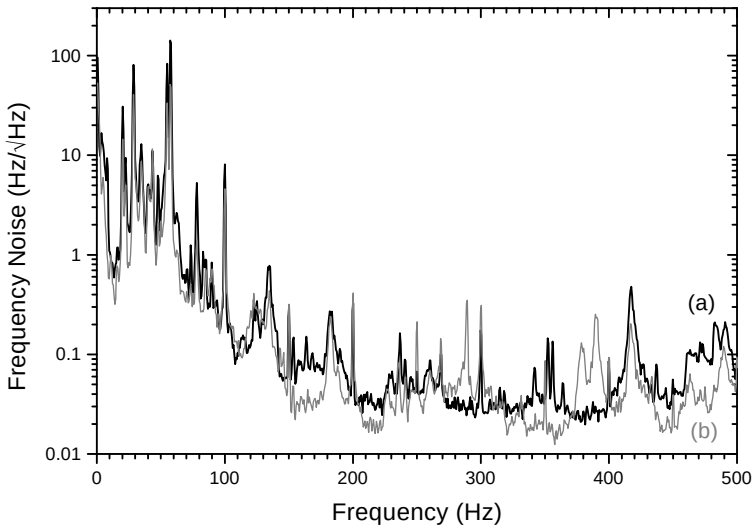

Fig. 8. Laser frequency noise: (a) in-air propagation; (b) in-fiber propagation. Frequency resolution: 0.6 Hz.

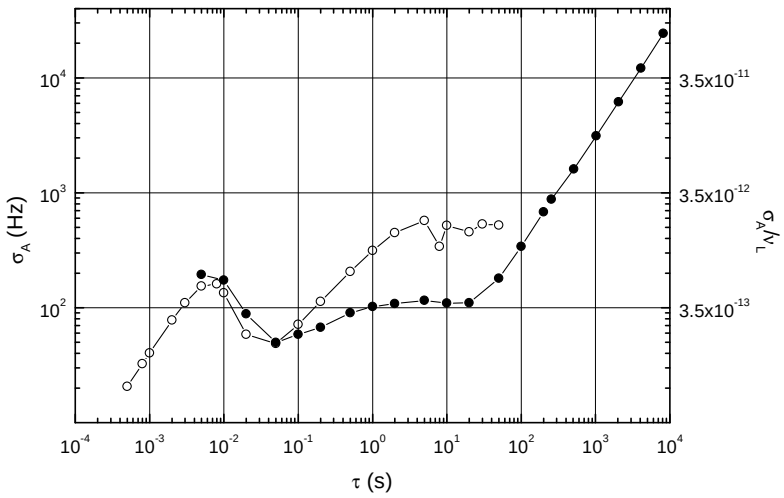

Fig. 9. Allan deviation of the stabilized laser. Closed circles: with no voltage applied to the PZT. Open circles: with offset voltage applied. The scale on the right gives the relative Allan deviation: σ_A/ν_L, where $\nu_L = 2.82 \times 10^{14}$ Hz is the laser frequency.